Scintillation Characterization for WAAS during Solar Maximum

Eric Altshuler, *Sequoia Research Corporation*
Karl Shallberg, *Zeta Associates Incorporated*
B. J. Potter, *LS Technologies*

BIOGRAPHIES

Dr. Eric Altshuler received his B.S. in mathematics and computer science from UCLA in 1989 and his Ph.D. in physics in 1998 from University of California at Irvine. He is currently a Senior Engineer at Sequoia Research Corporation. He is active in the development of Ionospheric Algorithms for WAAS and is a member of the WAAS Integrity Performance Panel. He has also worked on the HMI analysis for Multi-functional Satellite Augmentation System and the SLS-4000 Ground Based Augmentation System effort.

Mr. Karl Shallberg is a Senior Associate with Zeta Associates Inc. and currently is working GPS receiver performance and system engineering issues for the FAA GNSS Program. He previously was President of Grass Roots Enterprises Inc. and worked for the US Government. He received his B.S. in physics from Norwich University.

Mr. B. J. Potter has his bachelor's and master's degrees in electrical engineering from Oklahoma State University and the University of Minnesota. He now works with the Satellite Operations Group at the Mike Monroney Aeronautical Center in Oklahoma City. For more than six years he has monitored performance for, and investigated anomalous behavior in, the FAA's WAAS.

ABSTRACT

The primary development phases of the Wide Area Augmentation System (WAAS) occurred from 1996 through 2008, coincident with solar cycle 23 which peaked in 2002 and subsided in the 2005/2006 time frame. During that period, WAAS algorithms were under development and then tuned to account for several different ionospheric issues. The ionosphere related issues affecting WAAS performance include extreme storms (such as the "Halloween Storm" which occurred during October 29th through 31st of 2003) as well as extreme gradients (as was seen on November 20th and 21st, 2003). Those ionospheric threats, along with others, were extensively researched and the WAAS ionosphere related algorithms developed to mitigate such events. As solar cycle 23 subsided, WAAS ionospheric algorithms supported very good availability performance during the remainder of the cycle.

As solar cycle 24 activity increased during the 2009/2010 time frame, the WAAS ionospheric focus turned from the more extreme ionospheric phenomena seen previously to scintillation. Scintillation was certainly a phenomenon WAAS considered with its ionospheric research but the installation of additional reference stations in far northern Alaska and Canada as well as in Mexico made it clear that scintillation was occurring on a regular basis and so should be given more consideration. Phase scintillation is most prominent at northern latitudes while amplitude scintillation is prevalent in the Equatorial anomaly region, which is sampled by the southernmost stations in WAAS. While individual scintillation events have been noted and studied, no overarching study has been undertaken to examine the effects that scintillation has had on WAAS over a considerable time period.

This paper presents a detailed characterization of scintillation as seen by WAAS during the ascending peak of the present solar cycle 24 (early 2011 through the end of 2014). The paper examines the characteristics of scintillation events, noting the frequency, size, duration, geographic location as well as overall spatial extent. Tracking performance with respect to both L1 and L2 is also examined, specifically instances where carrier lock on one frequency is maintained while lock on the other is lost. These results are compiled over an approximate four year time period.

INTRODUCTION

The Wide Area Augmentation System (WAAS) is a safety critical system that augments the Global Positioning System (GPS) by providing additional ranging from geostationary earth orbit (GEO) satellites, improved accuracy with differential corrections, and safety with integrity monitoring. WAAS reached its initial operating capability in July 2003 and now consists of 38 reference stations, three master stations, and six uplink

stations supporting three L1/L5 GEO satellites. WAAS reference stations are located throughout the contiguous United States, Hawaii, Alaska, Puerto Rico and internationally with stations in Mexico and Canada.

The WAAS Program has focused significant attention since its inception on understanding the ionosphere for purposes of providing corrections along with appropriate bounds on these corrections. This effort has chiefly addressed large-scale ionospheric disturbances since these produce the primary threats that the system must mitigate. This paper examines ionospheric scintillation, which may be described as smaller scale and more localized. Scintillation is caused by inhomogeneities in the ionosphere that generate rapid, small scale fluctuations of either signal amplitude or signal phase. The impact of scintillation is degraded receiver tracking, resulting in increased potential for cycle slips or complete loss of signal tracking. Either of these causes WAAS algorithms to react in a negative and very conservative way, given the safety impacts associated with the WAAS mission.

The goal of this paper is to examine macroscopic characteristics of the ionosphere using a very high fidelity data set spanning several years during solar maximum. To this end, we examine geographic regional behavior, temporal behavior (both diurnal and annual), extent (both spatial and temporal) as well as various statistics.

DATA SET

The Federal Aviation Administration (FAA) group at the Mike Monroney Aeronautical Center in Oklahoma City is charged with operating and maintaining WAAS, and as such, has a significant repository of system data. This repository and the ability to process large volumes of measurement data were leveraged to span as much of the current solar cycle as feasible. The data set utilized for this scintillation characterization effort was from January 2nd, 2011 through January 31st, 2015. This spans approximately four years and, as shown in Figure 1, encompasses a significant part of solar cycle 24 [1]. For future reference in this paper, this translates to the beginning of GPS week 1617 until the end of GPS week 1829.

The WAAS data used for this effort were one second ranging and status data from the 38 WAAS reference stations. Each reference station has three independent processing threads consisting primarily of a reference receiver, cesium frequency standard, antenna, and data collection and processing computer. For this scintillation characterization effort, the measurement (satellite ranging) and status data were processed from all 114 of these independent threads for the four year span defined above.

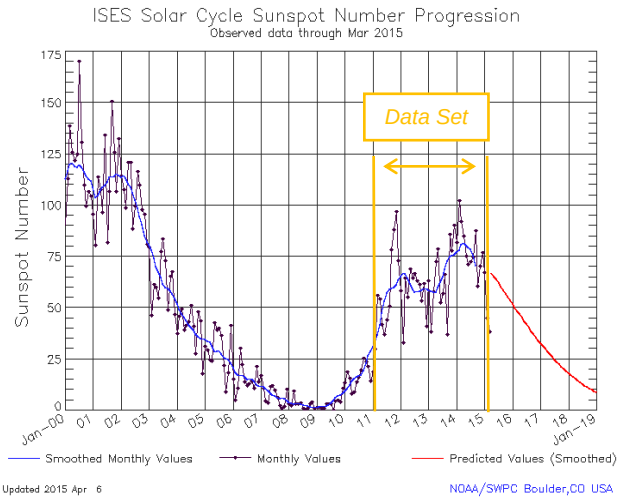

Figure 1 – Scintillation Data Set

WAAS REFERENCE STATION DATA PROCESSING

Processing WAAS reference station data to associate loss of tracking or cycle slips specifically to ionospheric scintillation activity required several steps. The processing needed to identify not only conditions where scintillation was impacting WAAS receiver tracking but also other conditions that result in the same effect. These other conditions are multipath fading, Radio Frequency (RF) interference [2], satellite maintenance outages, satellite "glitches" [3], station specific signal blockage, network communication outages, and marginal or failed reference station equipment (receivers, clocks, or antenna). Isolating tracking issues to scintillation and mitigating these other effects required processing individual receivers, comparing receiver tracking status across the three independent reference station receivers, and finally, making event associations across the entire network of WAAS receivers.

MEASUREMENT PROCESSING

The first processing step utilized an application that executed on one second reference station ranging measurements and automatic gain control (AGC) data on a per reference receiver basis. The key inputs to this application besides each receiver's data were station locations and GPS almanacs. The application used healthy satellites as indicated in weekly almanacs to determine if a satellite should be processed above an elevation mask at a given reference station. The elevation mask was critical to mitigate loss of lock or cycle slips that could be caused by site specific multipath. WAAS receiver tracking is generally very robust above 5 to 10

degrees elevation so the elevation mask for this processing was set conservatively at 20 degrees. Receiver L1 and L2 signal tracking was evaluated against predicted signal tracking from the GPS almanac and any instance of missing receiver signals recorded for future processing. The program also processed L1 and L2 carrier range in a manner similar to the WAAS operational software to detect cycle slips [4]. This processing performed a linear fit on the previous five seconds of L1 minus L2 carrier range measurements and projected forward to the current epoch for comparison with current carrier differences. If the residual from the check exceeded 0.055 meters, a cycle slip was recorded for the corresponding receiver/satellite pair.

The application performed additional processing to identify tracking issues caused by RF interference instead of scintillation. RF interference detection was accomplished with an algorithm that filtered L1 and L2 AGC measurements and flagged instances where current AGC estimates differed from filtered estimates by more than a specified amount. The filter time constant and RF interference detection threshold were determined based on field experience and were set conservatively to ensure tracking issues associated with interference were attributed correctly. Hysteresis of 120 seconds was added to the algorithm after RF interference subsided to account for satellite reacquisition time.

Figure 2 provides an example of L1 and L2 AGC processing for an interference event at the Miami / ZMA reference station. This interference was reportedly caused by a vehicle operating multiple Personal Privacy Devices (PPDs) in close proximity to the Miami Air Traffic Control Center. Figure 3 shows L1 and L2 signals not tracked above the mask during this RF interference (RFI) period. "RFI" in these Figures is the application flag indicating the presence of interference and that all missing satellite signals when this is set should be attributed to interference. Lastly, it is recognized that the 6 December 2006 X-Ray event would be attributed as RF interference with this processing approach because of receiver AGC response, but there were no similar ionospheric events observed in WAAS during the time period analyzed for this paper.

The application also computes metrics for carrier phase and C/No on a per satellite basis to further isolate tracking issues to phase or amplitude scintillation. This processing was thought to be needed originally to have some association of scintillation conditions when cycle slips and missing signals were identified. With the reasonability checks and voting described in the next section however, it was determined that these metrics were ultimately not needed to ensure events were attributed correctly.

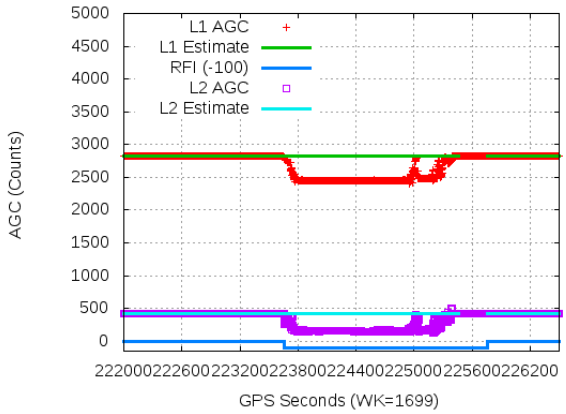

Figure 2 - ZMA-B: Example of AGC Processing during Significant RFI Event

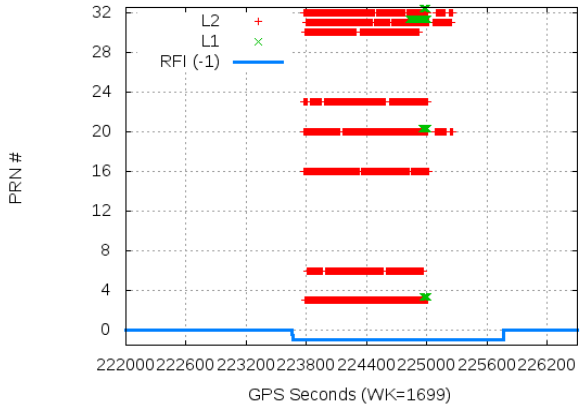

Figure 3 - ZMA-B; Example of RFI Monitor Flag and L1 and L2 PRNs not Tracked

REASONABILITY CHECKS AND VOTING

With the output of measurement processing from each station from the previous section, two major reasonability checks were imposed on these outputs to further isolate performance to scintillation. The first sought to determine satellite specific events by looking across stations to identify time periods in which a single satellite was not tracked at four or more stations for an extended length of time. Given the geographic diversity of WAAS reference stations and the line-of-sight attributes of scintillation, not tracking a satellite at the exact same instance at multiple stations would most likely be associated with a satellite issue (maintenance outage, glitch…etc.) and not scintillation. Thus, if a particular satellite was missing at four or more stations at any given epoch, the time period for this satellite event was defined by going forward and backward in time from this point to determine the entire outage period. The "satellite outage period" was then defined to be the total number of

consecutive seconds where this satellite was excluded from the measurement processing output. Consistently, the L2 frequency contained longer satellite outage periods than the L1 frequency so in order to be more conservative in the estimate of the duration scintillation events, the L2 exclusion time periods were used for both the L1 and L2 frequencies. An example of one such event is shown in Figure 4 with station count in red and culling period in magenta. The green line indicates that only one satellite was excluded during this period. On day two of GPS week 1617, PRN 4 was found to be missing for several hours with almost all stations in WAAS experiencing an outage for this satellite. Thus, this PRN was removed from the data set during this period since it clearly was not due to scintillation.

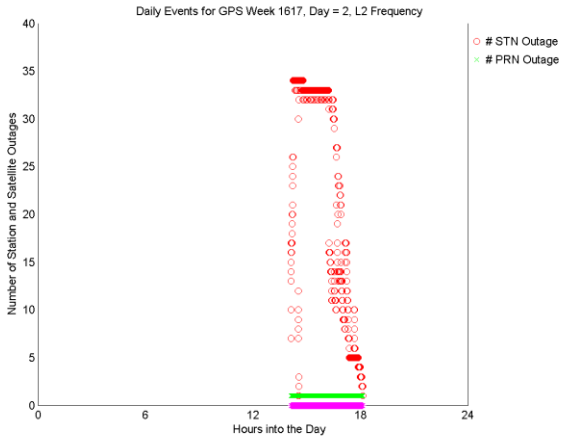

Figure 4 - Event for PRN 4, GPS week 1617

The other major reasonability check was defining line-of-sight blockage for each thread. While this issue does not necessarily occur daily, plotting azimuth and elevation for all missing signals at each reference station thread over several years reveals a recurring pattern of line-of-sight blockage. To prevent this type of data from being attributed to scintillation, a small azimuth/elevation window was defined for each thread in the system that exhibited this behavior and all missing signals or cycle slip events occurring within this window removed. An example of blockage can be seen clearly in Figure 5 for the A thread of Jacksonville / ZJX. Over the approximately two year span shown in the plot, the receiver experienced outages in the same (very narrow) azimuth and elevation window. For this particular receiver, the window was centered at 285.5° azimuth with ±2.5° on either side and 30.5° elevation with ±1.5° on either side. The band for each window is plotted in black. Any missing signals or cycle slips for which both azimuth and elevation fell within these bounds was removed, as it is clear that this data should not be attributed to scintillation.

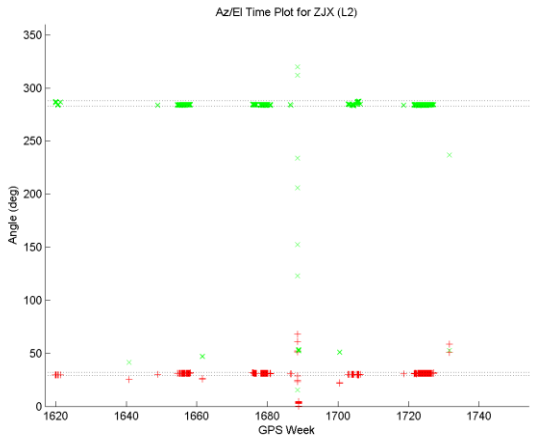

Figure 5 - Receiver/Satellite obstruction for ZJX-A

To this point in the processing, the identification of missing signals/cycle slips, RF interference association, multiple station outage, and azimuth/elevation blockage culling were carried out on A, B and C threads independently. Thus, the station data for each of WAAS's three threads were independently compiled and culled according to what has been discussed above, and similar data sets for each thread were created. While this process offers a significant reduction in non-scintillation events for each thread of data, looking across all three threads reduces erroneous events further. A voting step was therefore introduced across each set of three threads to create the final culled, voted scintillation data set.

The voting step is straightforward and assumes scintillation will produce similar responses across all three threads at a reference station. The exceptions to this assumption are the four stations that have receivers configured differently (discussed in the next paragraph) or instances when one of the threads has failed or marginal hardware causes receiver tracking issues. For each reference station then, the number of tracking events for each week was counted, and the thread with the minimum number of counts was used for that week for that station. The "final" data set is thus the collection of missing L1 and L2 signals and cycle slips represents the minimum number of events observed at each reference station over the four year period.

It should be noted that this voting was applied to all stations except Barrow / BRW, Kotzebue / OTZ, Iqaluit / YFB and Tapachula / MTP. To diversify carrier tracking at a reference station and hopefully mitigate some common mode carrier tracking errors, WAAS configured these four stations in late 2011 with different phase lock loop (PLL) bandwidth settings across the three threads. The receiver PLL bandwidth is a critical setting and dictates receiver tracking performance. The nominal WAAS PLL bandwidth is 3 Hz for L1, which is relatively narrow and is based on the desire to improve tracking in

low signal and/or high noise conditions. The weakness in this setting is greater susceptibility to loss of lock during high signal variation such as that experienced with phase scintillation. For these four stations, the A thread receiver was set to the nominal setting of 3 Hz, the B thread to 5 Hz, and the C thread to 7 Hz. The station results presented in the following sections for Barrow, Kotzebue, Iqaluit, and Tapachula are from the A thread only except where tracking differences between these stations are specifically analyzed.

ANALYSIS METRICS

For the analysis in the following sections, both L1 and L2 outages and cycle slips are examined. An outage in this context is the number of seconds in which the receiver was not tracking either the L1 or L2 signals. To ensure cycle slip detections were treated in a similar manner as L1 and L2 signal outages, each cycle slip was represented as a five second outage. The five seconds relates to the carrier phase accumulation required by the cycle slip algorithm to start its processing.

EQUATORIAL AND AURORAL BEHAVIOR

The final processed, culled and voted data set (which was described in the previous section) was analyzed to understand scintillation behavior in the WAAS network. One immediate observation was that there are two very distinct geographic regions for which the ionosphere causes significant tracking impacts in WAAS, namely the Auroral region in the north and the Equatorial region in the south. It should be noted here and throughout the paper that when the phrase "Equatorial Region" is used in the context of this study, it is meant to refer to the region north of the Equator, but still far enough south to sample the Equatorial Anomaly. It is very clear that the Equatorial and Auroral regions are separated by the mid-latitude region in which the ionosphere is benign to the point that there is virtually no impact to WAAS from stations located there. These observations can be seen clearly by plotting the total number of seconds of missing L1 and L2 signals over the data set as a function of magnetic latitude for the 38 WAAS stations, as shown in Figure 6. There are two WAAS stations in the Equatorial region at the lower magnetic latitudes (Hawaii / HNL and Tapachula / MTP) that encounter a significant number of outages. North of about 26° magnetic, the issues disappear even though there are several other WAAS stations located in Mexico, albeit at a higher magnetic latitude. There are virtually no issues from any station in the mid-latitude region, and the issues begin again at about 60° magnetic, becoming significant for the four stations above 65° magnetic (Kotzebue / OTZ, Fairbanks / FAI, Barrow / BRW and Iqaluit / YFB).

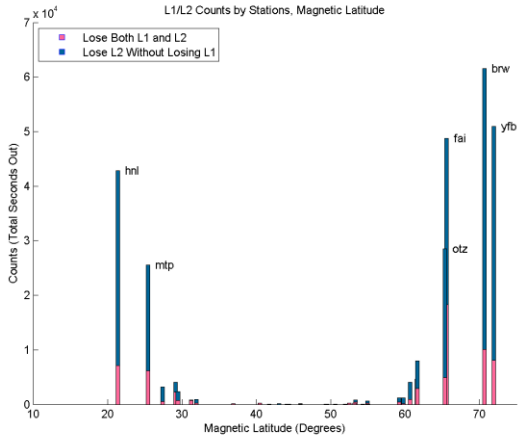

Figure 6 - Total number of seconds out plotted by WAAS station

The directional behavior of the Equatorial and Auroral regions is fundamentally different as well. The Equatorial stations in WAAS have issues when the satellite is south of the station due to the line of sight pointing directly into the Equatorial anomaly. The outages are virtually all attributed to an azimuth within about 30° of 180°, which is almost directly south. In contrast, the Auroral stations in WAAS encounter outages in all directions, and there is no "preferred" direction in which outages occur more frequently. This is illustrated in the two scatter plots shown in Figure 7. Figure 7a shows the azimuth/elevation scatter plot for Hawaii / HNL, which shows almost no outages except for azimuths between 150° and 210°, whereas Figure 7b shows that issues exist for all azimuths in the scatter plot for Barrow / BRW.

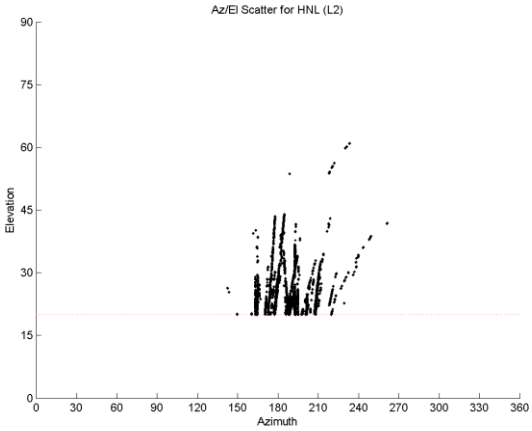

Figure 7a – Az/El Scatter plot for HNL

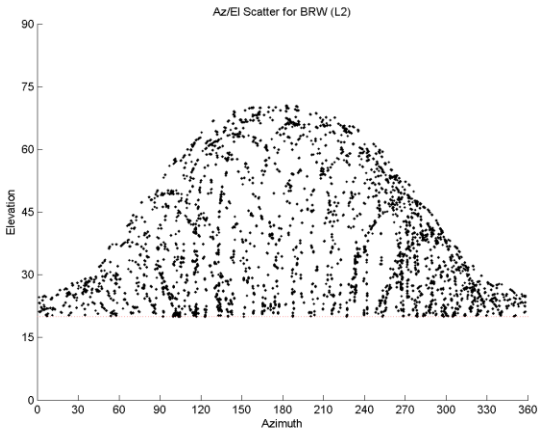

Figure 7b – Az/El Scatter plot for BRW

A scatter map plot of the L2 outages for the entire WAAS service region can be seen in Figure 8. It can be seen that the Hawaii / HNL and Tapachula / MTP stations in the south have their events occurring south of their location, whereas Barrow and Iqaluit both are surrounded by their outages. This is consistent with the scatter plots above in Figures 7a and 7b.

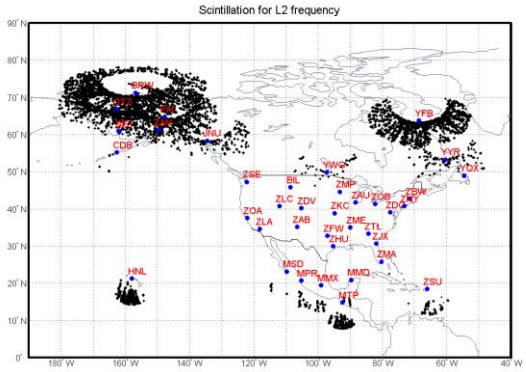

Figure 8 – Scatter map plot of L2 outages across the WAAS service region

The differences between the Equatorial and Auroral regions can also be seen when viewed across the data set plotted in time. To illustrate this behavior, the average number of cycle slip counts was computed over a 28 day window centered in each day of the data set, and plotted over the entire time span of the data set. Figures 9, 10 and 11 show the number of mean cycle slips over the entire four years of the data set, with red vertical lines as year boundaries and blue vertical lines as equinox/solstice boundaries.

The behavior in the Equatorial region can be seen most clearly by examining the behavior of Hawaii / HNL in Figure 9. The major peaks occur about six months apart and correspond to the Northern Hemisphere's late winter and late summer period. The behavior is primarily driven by the modal behavior of the equatorial anomaly and corresponds strongly to the equinoxes.

It is interesting to note that the relatively low ionospheric activity during 2013 corresponds to a dip in the solar cycle that can be seen in Figure 1. It could thus be conjectured that as the solar cycle continues to subside, the cycle slip activity will significantly decrease.

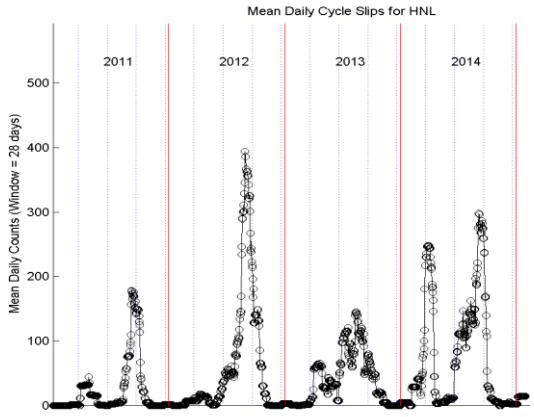

Figure 9 – Mean cycle slips for HNL for 2.6 years

The behavior of Barrow / BRW shown in Figure 10 is in stark contrast to the behavior of Hawaii / HNL for two fundamental reasons. First, there are no peaks that correspond to a one-year cycle and second, Barrow has an underlying background that never drops below about 100 cycle slip counts per day. In contrast, Hawaii / HNL exhibits long periods of time where the mean number of cycle slips approaches zero.

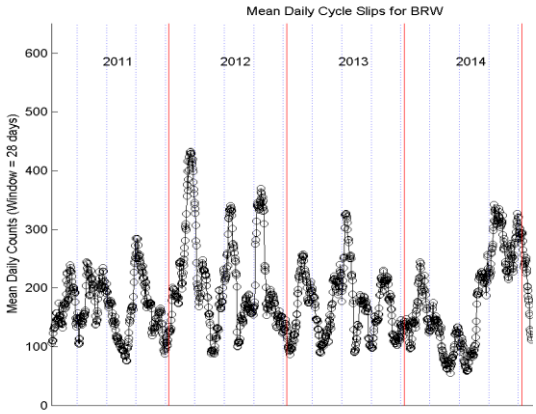

Figure 10 – Mean cycle slips for BRW over 2.6 years

Examining space weather data for the same time period reveals the planetary K index (K_p) relates to the major peaks in the Auroral region. As K_p is a quasi-logarithmic measurement, the K_p data was converted to its direct

measurement counterpart (referred to as A_p) and averaged in the same way as the cycle slip data, i.e., a 28-day moving window averaged over the time period. The entire A_p curve was then shifted down to remove the overall median value, so that the plotted peaks would appear more prominent, as can be seen in Figure 11.

The mean number of cycle slips was computed for the entire Alaskan region (Auroral Northwest contains stations Barrow, Kotzebue, Fairbanks, Bethel, Anchorage, Juneau and Cold Bay) and the mean A_p index (described above) was then overlaid and scaled so that the maximum of the peaks in the A_p data was the same as the maximum number of mean cycle slips. Figure 11 shows a strong correlation between the onset of peaks caused by ionospheric space weather and the number of cycle slips in the Auroral region. For every major peak, and many of the minor peaks shown in Figure 11, the onset of excessive ionospheric plasma corresponds to an increase in the average number of cycle slips. Note that the two curves in Figure 11 are not meant to be correlated numerically, but to simply show visually that these two phenomena are strongly coupled in time. The Equatorial region shows no such correlation.

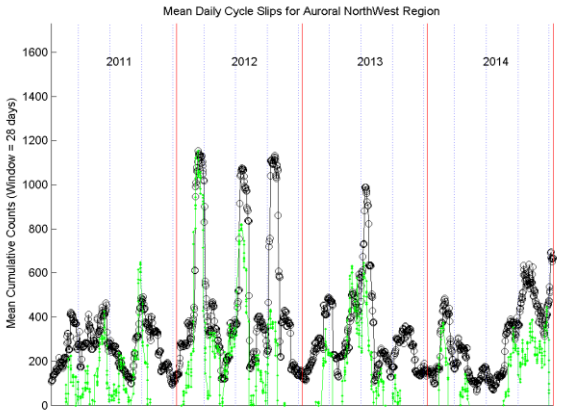

Figure 11 – Mean cycle slips and scaled A_p in Auroral Northwest for four years

It can be concluded that the behavior of the WAAS stations in the Equatorial and Auroral regions are driven by fundamentally different mechanisms. The stations in the Equatorial region experience issues primarily driven by the annual or semi-annual inflation of the Equatorial anomaly, whereas the stations in the Auroral region are primarily driven by excessive ionospheric activity during any season, and experience (roughly) daily issues.

FREQUENCY OF SCINTILLATION FOR WAAS

As the behavior for the Equatorial and Auroral regions have been characterized above, it is logical to next determine how often this behavior affects WAAS and in what capacity. To determine the percentage of days and the number of satellites affected, a windowing algorithm was applied to the cycle slip data. The windowing algorithm examined successive (one second at a time) blocks of data of 100 seconds over a day, and then recorded the total number of cycle slips in each block (if any), the number of unique stations associated with slips during that 100 second period, and the unique number of satellites associated with slips during that 100 second period. Thus, for each day, a set of "window statistics" were generated. This was conducted for the data set as a whole, regional data sets (both Equatorial and Auroral) and each individual station. Each day then has a "maximum number of unique satellites" and a "maximum number of unique stations", which are the most satellites or stations found in any 100 second time period on that given day. For some days, this number is zero as no tracking issues were recorded for that given day.

To show the percentage of days in which WAAS was affected by scintillation, the windowed data are plotted as a normalized histogram in which the number of satellites and stations is at least one (Figure 12). To add more information to the plot, the days were separated by the maximum number of satellites and plotted as a stacked bar chart, with the maximum number of PRNs separated by color. The height of each color represents the percentage of days for which that particular maximum number of satellites was out, and the total height represents the total percentage of days in which one or more satellites had cycle slips.

Only the most affected stations in each region are shown, with the Equatorial stations on the left half of the plot and the Auroral stations on the right half of the plot.

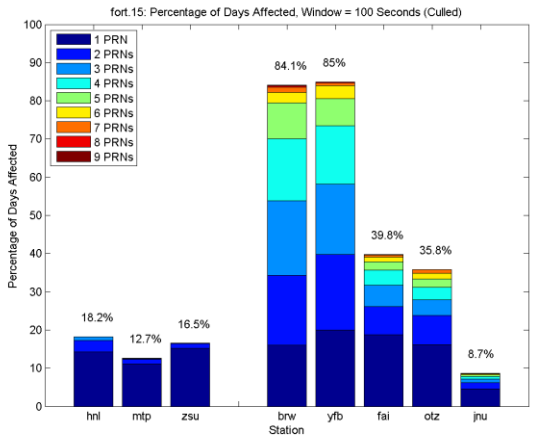

Figure 12 – Percentage of days affected for Equatorial and Auroral stations

As can be seen in Figure 12, the Auroral region is much more affected than the Equatorial region, both in percentage of days and maximum number of satellites impacted. The largest percentage of days is less than 20% for the Equatorial region but more than 80% for the Auroral region. For the Equatorial region, the number of satellites affected rarely exceeds two, possibly having to do with the unidirectional nature of the scintillation issues. For the Auroral region, the maximum number of satellites often reaches four or five. The data for the individual stations in a particular region can be combined into a regional data set, to yield a percentage of days affected for the region as a whole. It can be seen in Figure 13 that over 90% of the days in the data set are affected by scintillation in the Auroral region whereas only about 36% of the days are affected in the Equatorial region. Furthermore, the most likely number of satellites out in the Auroral region is four, whereas in the Equatorial region the most likely number of satellites affected is only one.

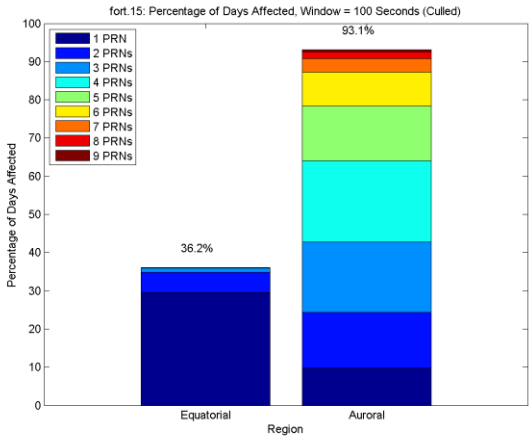

Figure 13 – Percentage of days in Equatorial and Auroral regions affected by cycle slips.

Similar behavior can be seen when the same windowing algorithm is applied to the number of days that experience L2 outages, as is shown in Figure 14. While for both regions the percentage of days is less for L2 outages than for cycle slips, it can be seen that the signal is lost on a significant number of days.

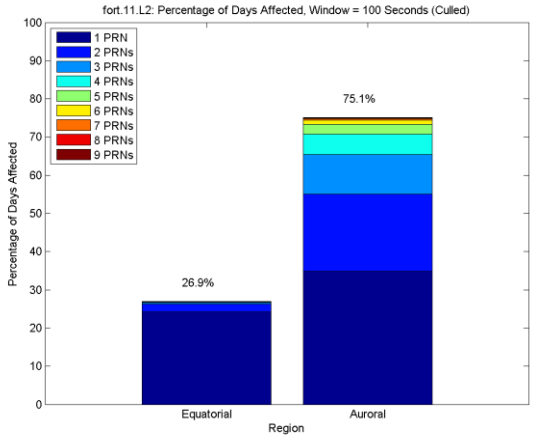

Figure 14 – Percentage of days in Equatorial and Auroral regions affected by L2 outages.

The previous plots might suggest that WAAS users are constantly affected by scintillation, however it can be shown that while the significant percentage of days affected by scintillation is relatively high, the impact is experienced for only a few hours a day. As with the previous analysis, the Auroral and Equatorial regions showed markedly different behavior. To demonstrate this, the cycle slip counts were adjusted to local time and plotted in a histogram and complied over the stations from Figure 12. The results for the Auroral region and the Equatorial region can be seen in Figure 15 and Figure 16 respectively.

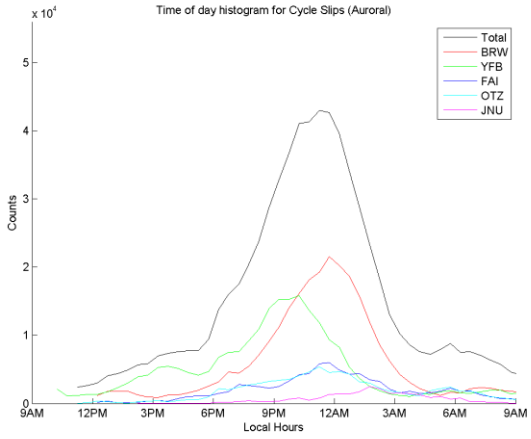

Figure 15 – Local Time Distribution for Cycle Slips in the Auroral Region

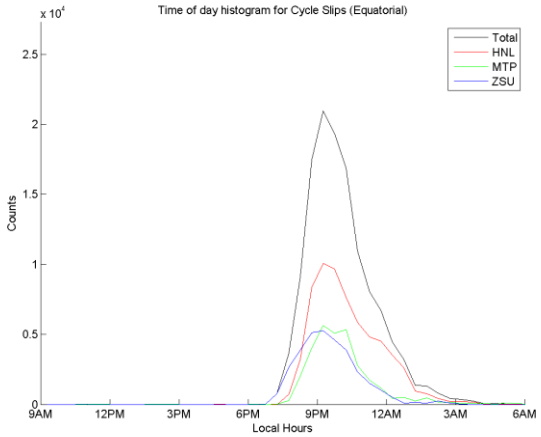

Figure 16 – Local Time Distribution for Cycle Slips in the Equatorial Region

The peaks for both the Auroral and Equatorial time of day histograms are both unimodal, and thus simple statistics can be generated that show the behavior of the mean local time of the central peak, as well as the duration of the impact periods. The mean local time of the peak was determined by taking the first moment of the distribution centered at the maximum, and the "width" (or duration) was computed by performing a "full width at half maximum" algorithm. As can be seen in Figures 15 and 16, the period of time of impact is a short fraction of the day. It can also be seen that the Auroral region is impacted for roughly two to three times the length of time as the Equatorial region. The L1 and L2 frequency outage distributions look very similar to the cycle slip distribution. A full set of statistics for the cycle slips, the L1 outages and the L2 outages are shown in Table 1.

Table 1 – Average Daily Impact Times and Durations

	Auroral		Equatorial	
	Local Time	Duration	Local Time	Duration
Cycle Slips	22:59	6:15	22:10	2:41
L1 Outages	22:43	4:08	21:35	1:14
L2 Outages	22:50	5:19	21:44	1:50

SPATIAL SCINTILLATION EXTENT

While the previous results show the ubiquity of scintillation throughout the four years of data, it is interesting to focus on the extent and simultaneity of a major scintillation event. A useful example of the behavior to be characterized can be observed with cycle slip detections from stations located in Alaska on July 15th, 2012. Figure 17 shows the breakdown of cycle slip indications for this day for each of the seven stations in this Auroral Northwest region. The figure shows cycle slip indications for each GPS PRN by time of day (UTC) for each of the stations, where the Y offsets of the blue dots within one of the station bands are scaled by the PRN number, ranging from 1 to 32, with 32 being at the top of the band. Other than Cold Bay (which has no events), the stations experience multiple events over multiple satellites over a significant portion of the day. This data can be further reduced by counting the unique number of WRS, of PRN, and affected tracks happening at a given instant. This reduction is shown in Figure 18.

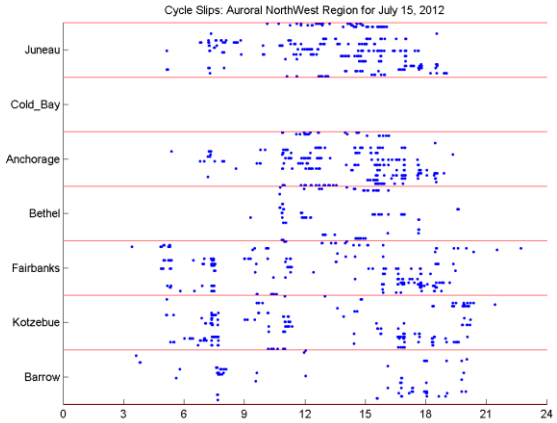

Figure 17 – Scatter plot of events in the Auroral Region for July 15th, 2012

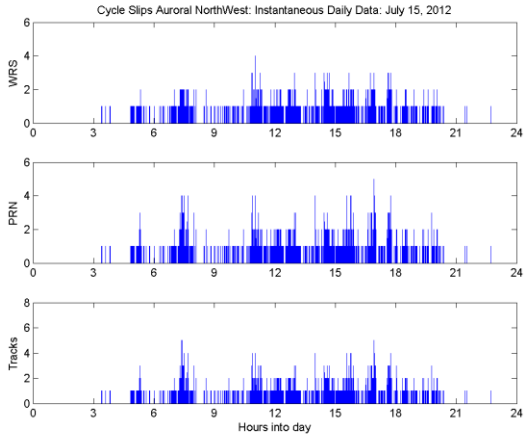

Figure 18 – Instantaneous events for July 15th, 2013

The data set in Figure 18 shows that there are periods of time in which four stations (of seven) are impacted and other periods of time in which four or five satellites are impacted. However, the one-second resolution of the plots above does not clearly illustrate that there are periods of time in which scintillation has a more significant effect than other periods. In order to better show this phenomenon, a ten minute windowing algorithm was applied to the data. The statistics for each time step were

computed using all of the data within the previous ten minutes. The results are shown in Figure 8 below.

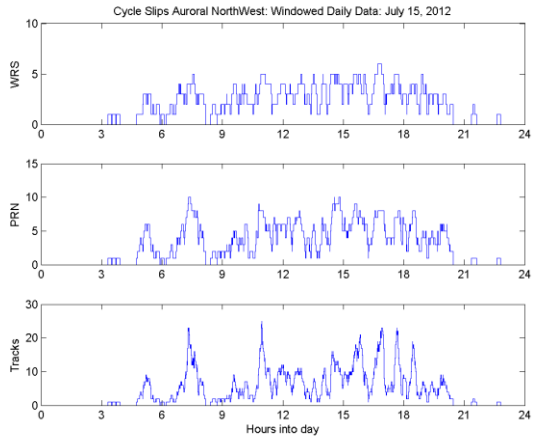

Figure 19 – Windowed events for July 15th, 2012

As can be seen in Figure 19, the maximum number of stations impacted in a ten minute window was six, which is all of them except for Cold Bay. Also, the maximum number of satellites that were impacted is ten, and the maximum number of tracks (unique station/satellite pairs) that were impacted is 25. More to the point, the three time series above show that there are periods of the day much more affected than others, which is difficult to imply from the instantaneous times series in Figure 18. These periods appear to last for about an hour, and occur several times throughout the day.

This event on July 15th, 2012 was somewhat extreme and scintillation was present for an extended period over this day. What is clear is that there are periods of time in which major sections of the region are affected. Thus, when one satellite is affected, it implies that more (maybe many more) are affected. It is also apparent that there are short periods of time in which several stations and satellites are impacted at the same time.

It is interesting to examine how many days in which multiple reference stations are impacted with cycle slip indications similar to the July 15th event. Three levels of satellite degradation were assessed across the stations in the Auroral Northwest, namely when one or more satellites were affected, when three or more satellites were affected and when six or more satellites were affected. Using the entire four year data set, the maximum number of stations impacted on a given day is plotted for the three different levels of satellite outages in Figure 9. Note that the data in Figure 20 represents dates when multiple stations are affected, which is why there is no data showing that a single station is ever affected. This is done intentionally, as the goal is to identify dates in which scintillation is somewhat widespread.

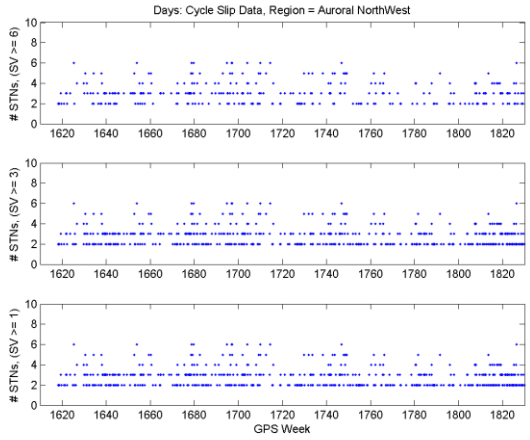

Figure 20 – Time series of station outages for different SV levels, Auroral Northwest Region, Cycle Slip data

As can be seen in Figure 20, the data set regularly shows multiple station (two or more) degradations, and moreover, there are many days in which six or more satellites were impacted, accompanied by most of the stations in the region being affected as well. A histogram of the different satellite cycle slip indications shows an interesting result; that in the event of multiple stations being impacted, if one satellite is affected, then more than likely more than one satellite will be affected. This can be seen below in Figure 21.

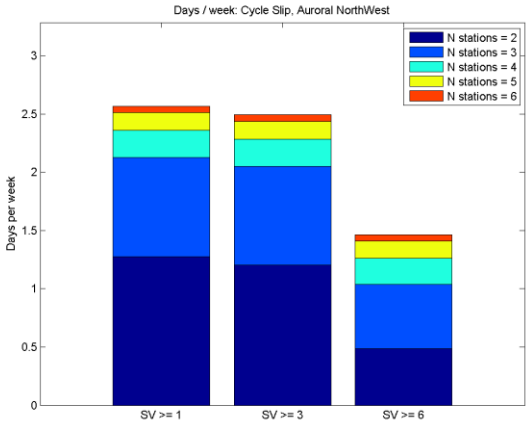

Figure 21 – Number of days per week of cycle slips for the Auroral Northwest

Cycle slip indications on one satellite at two or more stations almost directly imply impacts on three satellites at multiple stations. This is a striking result in that it implies that scintillation in the Auroral region is highly correlated and has a very large spatial extent. Also, cycle slip indications on one satellite imply a better than 50% chance that six will also be affected. As the plot above shows, roughly 2.5 days of 7 are affected so the expectation is roughly 1/3 of the days at least one satellite

and two stations will be impacted in the Auroral region near the peak of a solar cycle. Additionally, about 1/5 of the time at least six satellites and at least two stations will be impacted.

For comparison purposes, regions were defined for the other stations shown to experience scintillation. The Auroral Northeast was defined by reference station performance at Iqaluit, Goose Bay, Gander and Winnipeg and the Mexico Region was defined by performance at Tapachula, San Juan, Merida, Mexico City, Puerto Vallarta, San Jose del Cabo and Miami. The correlation observed with the Auroral Northwest is true for the Auroral Northeast as well, as can be seen below in Figure 22. This region has fewer stations (only four), but the same basic satellite behavior is observed, i.e., cycle slip indications on one satellite implies affecting three, and impacting one or three implies about a 50% chance of affecting six.

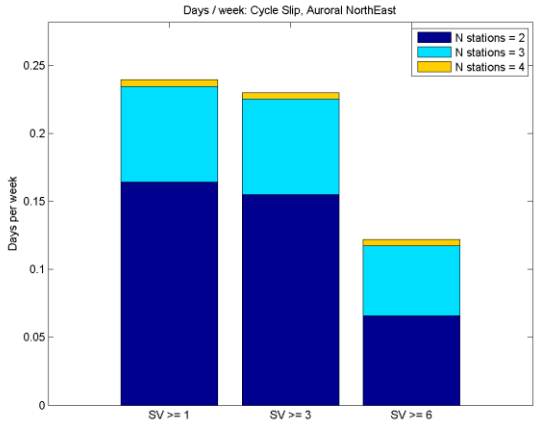

Figure 22 – Number of days per week of cycle slips for the Auroral Northeast

In contrast, the Mexican region, which has the same number of stations (seven) as the Auroral Northwest, has far fewer events in it, as shown in Figures 23 and 24.

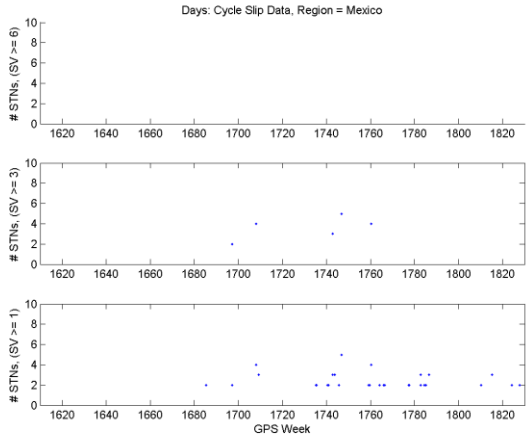

Figure 23 – Station Outage for different SV levels, Mexico Region

The same type of histogram has been plotted for the Mexican region in Figure 24 below. Not only are the number of days far fewer, but the behavior is fundamentally different. Cycle slip indications on one satellite does not imply affecting three, and six satellites were never lost in the entire four years of data.

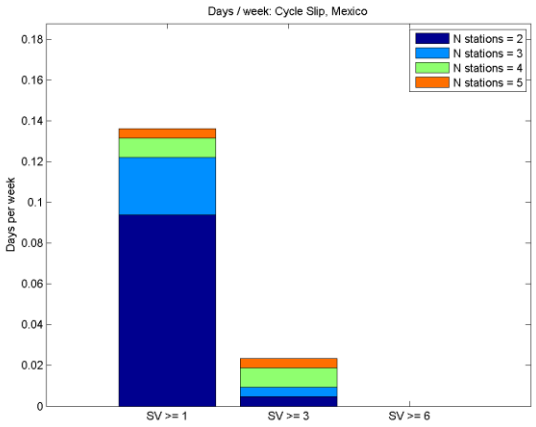

Figure 24 – Number of days per week of cycle slips for Mexico

The results thus far used cycle slip indications, which are more abundant than either L1 or L2 outages from complete loss of tracking. The same characterization was conducted with loss of L1 and L2 tracking for the Auroral Northwest region. As expected, the L2 frequency is much more susceptible to outages than L1. The L1 outages never rise above three stations out at any one time, but the L2 outage data increases to five on some occasions. The actual number of days with outages is contrasted as well. The numbers of days out, broken down by number of stations out for the three satellite outage levels, are shown as time series in Figures 25 and 26, and then again as histograms in Figures 27 and 28. As can be seen, L2 has

about three times the number of days affected than L1. This is true for all levels of satellite outages.

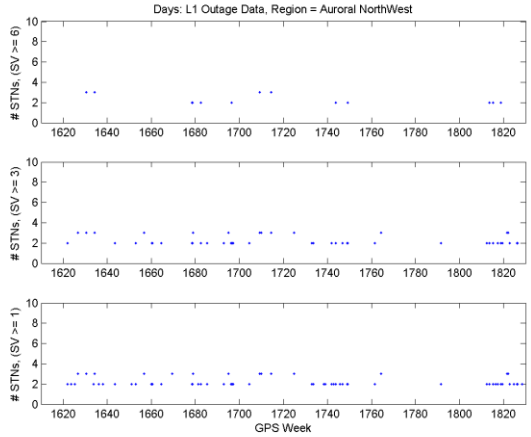

Figure 25 – Time series of station outages for different SV levels, Auroral Northwest Region, L1 outage data

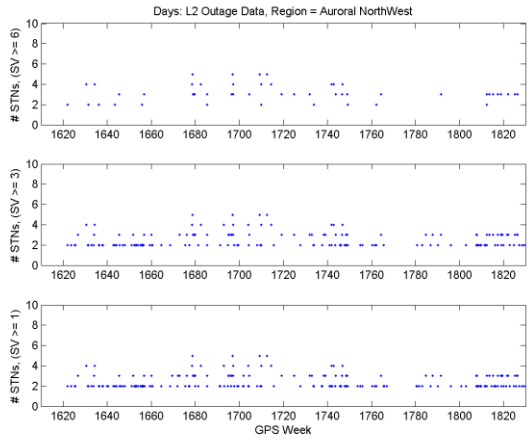

Figure 26 – Time series of station outages for different SV levels, Auroral Northwest Region, L2 outage data

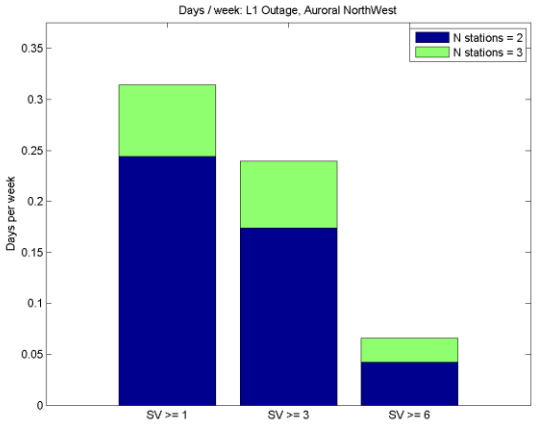

Figure 27 – Bar Chart of station outages for different SV levels, Auroral Northwest Region, L1 outage data

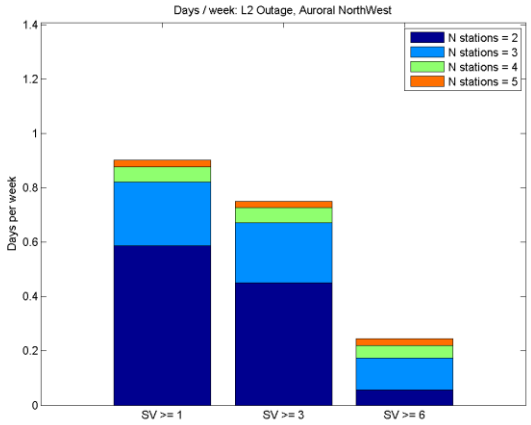

Figure 28 – Bar Chart of station outages for different SV levels, Auroral Northwest Region, L2 outage data

SPATIAL EXTENT CHARACTERIZATION

The result that several stations and/or satellites can be affected in a short period of time by cycle slip indications leads to the question of how geographically large a scintillation event is. As might be expected, the results are highly dependent on the amount of time used to collect the events. A short trade study was conducted on four different time windows of 0, 10, 20 and 30 minutes for the Auroral Northwest, for days that have at least two stations and two satellites affected at the same time. The geographic extent was computed by collecting cycle slip data over the window of time, computing the convex hull of the data, dividing it into geodetic triangles and then computing the area of the IPP projected onto the surface of the earth. The dates used are the same dates shown in Figure 20 and there are 407 dates out of 1190 which meet the criteria. The results of these computations are shown in the time series in Figure 29 below.

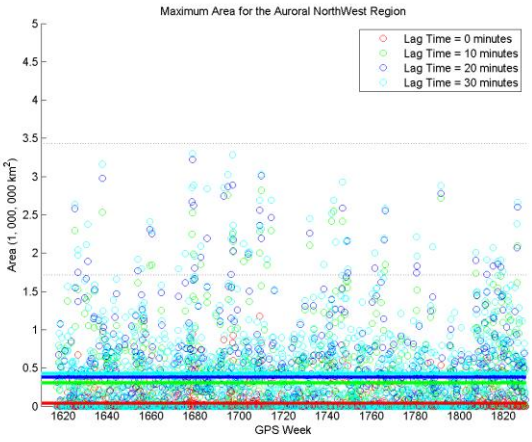

Figure 29 – Spatial Extent as a function of day in the Auroral Northwest

The colored circles represent the computed spatial extent in millions of square kilometers. The colored horizontal lines are the average of the circles, excluding the instances of zeros. As can be seen by the horizontal red line in the figure above, the instantaneous spatial extent is very low, however collecting data for even ten minutes creates a very large spatial extent, as can be seen in the green horizontal line. Adding more time does not increase the average much, as can be seen in the blue and cyan lines. For comparison, the area of Alaska is about 1.7 million km^2, and increments of this number are plotted as horizontal black dotted lines.

To obtain a greater appreciation for geographic size and relative probabilities of scintillation impacts, the spatial extent computation was run on the entire data set for all three regions (Auroral NW, Auroral NE, and Mexico), for all four window times. Figures 30, 31 and 32 below show the histogram for the spatial extent for the three different regions, for the four different window times. The area of Alaska is plotted as a red line for reference. Note that due to the large number of days with zero events, the Mean Area is computed using the non-zero data.

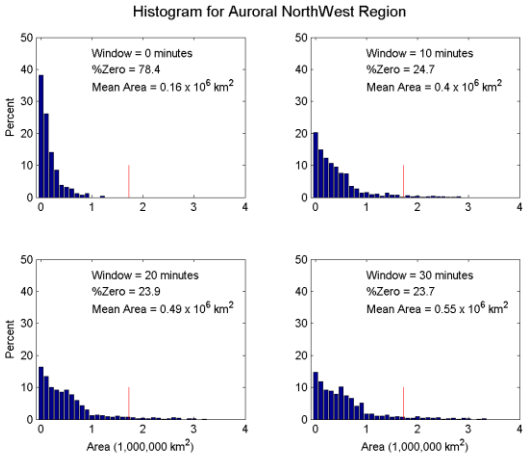

Figure 30 – Spatial Extent Histogram for the Auroral Northwest Region

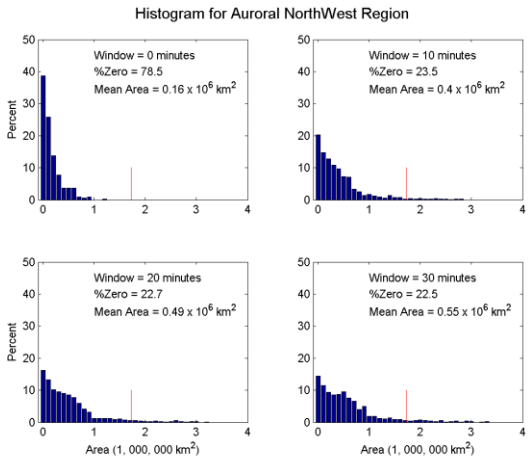

Figure 31 – Spatial Extent Histogram for the Auroral Northeast Region

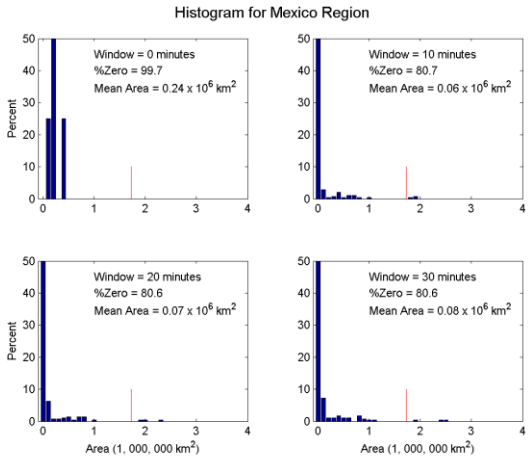

Figure 32 – Spatial Extent Histogram for the Mexico Region

As can be seen, using a window changes the statistics in all three regions, but as previous results suggested, the difference between a 10, 20 or 30 minute window is relatively little. The Auroral Northwest is the region with the largest distribution. On about 75% of the days, on average, there is an impacted area of ½ million square kilometers, which is about 1/3 the size of Alaska. Furthermore, there are several dates for which the impact exceeds the size of Alaska, and even gets close to twice the size of Alaska. This represents a significant spatial extent for users in this region. The Auroral Northeast shows comparable, albeit slightly smaller results. In contrast, the Mexico region has a much higher percentage of days where no activity is recorded, and when there is activity, the spatial extent is much smaller.

The results above show a clear and consistent picture. Scintillation in the Auroral region is a very large phenomenon which covers a very wide geographic extent. Furthermore, it appears that severe scintillation occurs in bursts, where the time periods for particular phases of the

event are on the order of an hour or so. The Auroral region findings are in stark contrast with the data from the Mexican region, which shows a much smaller effect, both in frequency and spatial extent.

It should be noted that there are some limitations in this analysis due to inhomogeneity of the WAAS station placement. First, the spatial extent analysis is limited by the size of the cluster, and the actual spatial extent is likely even larger than reported here. Second, the Mexican region is only analyzed with stations that are located on the edge of the equatorial anomaly, and as such, may not be adequately describing the spatial extent of scintillation in the Equatorial region.

CONCLUSIONS

Examination of WAAS tracking and cycle slip performance associated with scintillation demonstrates distinct impacts for both the Equatorial and the Auroral regions. The ionospheric mechanisms which drive the behavior in these two regions seem to be fundamentally different. The Equatorial region appears to be driven by the behavior of the Equatorial anomaly, which is well understood and follows a seasonal cycle. In contrast, the Auroral region appears to be driven by periods of excess ionospheric plasma, i.e., periods of high K_p, whenever they may happen throughout the year. Furthermore, at least some amount of scintillation occurs on roughly a daily basis in the Auroral regions. However the Equatorial regions encounter scintillation issues much less frequently.

The geographic spatial extent of scintillation events in the Auroral region can become very large, which leads to very significant, correlated (simultaneous) satellite outages. The areas of the scintillation events are measured relative to the area of the state of Alaska. On average, the affected area is about 1/3 of the area of Alaska, but can get close to twice the area for particularly large events. This size and regularity of scintillation events leads to highly correlated satellite impacts in the Auroral region. About 1/3 of the days have two or more stations and 3 or more satellites impacted, and about 1/5 of the days has two or more stations and 6 or more satellites impacted. Furthermore, it is very rare that a single satellite is affected without multiple satellites being impacted.

The occurrences of scintillation for WAAS were found to be significant but the impact to WAAS integrity has been shown to be mitigated, and the impact to performance (coverage) appears negligible. Nevertheless, mitigation strategies do exist that could make WAAS more robust to scintillation and these may have additional benefits of lessening the impact of satellite related outages.

ACKNOWLEDGMENTS

The authors would like to acknowledge that this effort was sponsored by the FAA satellite program office.

REFERENCES

[1] http://www.swpc.noaa.gov/SolarCycle/
[2] B. J. Potter, et. al., “Personal Privacy Device Interference in the WAAS”, GNSS ION Sep. 2012
[3] S. Gordon, et. al., “PRN-21 Carrier Phase Perturbations Observed by WAAS”, GNSS ION Sep. 2009
[4] K. Shallberg, S. Fang, “WAAS Measurement Processing; Current Design and Potential Improvements”, PLANS 2008
[5] RTCA Special Committee 159 Working Group 2, “Minimum Operational Performance Standards for Global Positioning System / Wide Area Augmentation System Airborne Equipment,” RTCA Document Number DO-229D December, 2006.